MICROSTRUCTURAL ANALYSIS OF A GLASS DEDICATED TO THE RADIOACTIVE WASTE CONFINEMENT BY RAMAN AND FTIR SPECTROSCOPY**

D. Moudir [1*], N. Kamel [1], Y. Mouheb [1], A. Sadji [2], Y. Hamiane [2]

[1] Algiers Nuclear Research Centre, Division of Nuclear Techniques, Alger-RP, Algiers, Algeria; e-mail: dalilamoudir@yahoo.fr
[2] Polytechnic National School of Constantine, New University City Ali Mendjeli, BP 75, A, New city RP, Constantine, Algeria

This study deals with the structural changes occurring in a Mo-reach glass dedicated to the confinement of Mo-reach radioactive waste that contains different contents of Cs_2O oxide, ranging from 0.3 to 0.6 wt.%. The glass synthesis was carried out by the double melting method at 1380°C, followed by a stage of 2 h at 600°C. Neodymium was an actinide simulator. The glasses were characterized by their physical and microstructural properties using different spectroscopic techniques. As the experiment shows, the glass geometrical density varies between 1.96 and 2.75g/cm^3. X-ray diffraction (XRD) analysis shows amorphous features, with traces of crystalline germs, identified as the $CaMoO_4$ powellite phase, which probably formed during glass cooling. Fourier transform infra-red (FTIR) analysis reveals the main chemical bounds in the glasses: Si-O-Si and O-Si-O in SiO_4, B-O-B in BO_3, and Al-O-Al in AlO_4. The addition of Cs_2O raises the rate of polymerization in the glass network and then decreases the number of no-bridged oxygens (NBO). Raman spectroscopic analysis reveals the absorption bands of MoO_4^{2-} in $CaMoO_4$. It shows that the Mo environment is altered by the addition of increasing contents of Cs_2O in the glass. This is evidenced by the absorption bands shifts at 319, 792, and 844 cm^{-1}. The absorption band located at 700 cm^{-1}, ascribed to the elongation of SiO_4 and AlO_4, is attenuated for 0.4 and 0.6% of the Cs_2O content. It shifts to 680–900 cm^{-1} due to the glass high Mo content but increases in intensity with the Cs_2O content, thus disturbing the alkali positions of Ca and Na, with Cs remaining soluble in the glass. One can conclude that a little rise in the Cs_2O content inhibits the phase separation of both Na and Ca molybdates. The glasses analyses do not show particular changes in the lanthanide valences, which are probably in a +III oxidation state. The addition of Cs_2O in this kind of glass network remains an issue with respect to the coherence of its microstructure. However, about 0.6 wt.% of Cs_2O has been incorporated in the glass network, with no Cs_2O phases segregation.

Keywords: *nuclear glass, Mo, Cs, Raman, Fourier transform infra-red analysis, X-ray diffraction.*

МИКРОСТРУКТУРНЫЙ АНАЛИЗ СТЕКЛА, ПРЕДНАЗНАЧЕННОГО ДЛЯ ЛОКАЛИЗАЦИИ РАДИОАКТИВНЫХ ОТХОДОВ, МЕТОДАМИ КОМБИНАЦИОННОГО РАССЕЯНИЯ СВЕТА И ИК-ФУРЬЕ-СПЕКТРОСКОПИИ

D. Moudir [1*], N. Kamel [1], Y. Mouheb [1], A. Sadji [2], Y. Hamiane [2]

УДК 543.42;535.375.5

[1] Алжирский центр ядерных исследований, Алжир; e-mail: dalilamoudir@yahoo.fr
[2] Политехническая национальная школа Константины, Университетский городок Али Менджели, Константина, Алжир

(Поступила 21 декабря 2020)

Исследованы структурные изменения в молибденовых стеклах с содержанием Cs_2O 0.3–0.6 мас.%, предназначенных для локализации радиоактивных отходов. Синтез стекол проведен методом двойного плавления при 1380 °C с последующим отжигом при 600 °C. Неодим – симулятор

**Full text is published in JAS V. 89, No. 1 (http://springer.com/journal/10812) and in electronic version of ZhPS V. 89, No. 1 (http://www.elibrary.ru/title_about.asp?id=7318; sales@elibrary.ru).

актинида. Физические и микроструктурные свойства стекол охарактеризованы с помощью различных спектроскопических методов. Геометрическая плотность стекол 1.96–2.75 г/см^3. Рентгеноструктурный анализ показывает аморфные особенности со следами кристаллических зародышей, идентифицированных как фаза повеллита $CaMoO_4$, которые образуются во время охлаждения стекла. ИК-Фурье-анализ выявляет основные химические связи в стеклах: Si-O-Si и O-Si-O в SiO_4, B-O-B в BO_3 и Al-O-Al в AlO_4. Добавление Cs_2O увеличивает скорость полимеризации стекла, а затем снижает количество атомов кислорода без мостикового соединения. КР-спектроскопический анализ выявляет полосы поглощения MoO_4^{2-} в $CaMoO_4$. Окружающая среда Mo изменяется при добавлении Cs_2O в стекло, о чем свидетельствуют смещения полос поглощения при 319, 792 и 844 см$^{-1}$. Полоса поглощения при 700 см$^{-1}$, приписываемая удлинению SiO_4 и AlO_4, ослабевает при содержании Cs_2O 0.4 и 0.6 % и сдвигается до 680–900 см$^{-1}$ из-за высокого содержания в стекле Mo, однако с ростом содержания Cs_2O увеличивается по интенсивности, нарушая щелочные позиции Ca и Na. Cs остается растворимым в стекле. Таким образом, небольшое увеличение содержания Cs_2O ингибирует фазовое разделение молибдатов Na и Ca. Анализ стекол не показывает особых изменений валентностей лантаноидов, которые находятся в степени окисления +III. Добавление Cs_2O в стеклянную сетку такого вида остается проблемой согласованности ее микроструктуры. При этом ~0.6 мас.% Cs_2O включено в сетку стекла без сегрегации фаз Cs_2O.

Ключевые слова: *стекло для локализации радиоактивных отходов, Mo, Cs, спектроскопия комбинационного рассеяния света, инфракрасная спектроскопия с преобразованием Фурье, дифракция рентгеновских лучей.*

Introduction. Radioactive substances exist in the environment, but they can also be of human origin. They have numerous beneficial applications that extend from electricity production to the medical, industrial and agricultural applications, including the extraction and processing of both uranium and thorium ores. These activities generate radioactive waste of various forms (gaseous, liquid, and solid) [1]. It is crucial to safely manage this waste, to ensure both people and environment protection, and to avoid their becoming a burden for future generations. Many waste storage processes employ glass as a confinement material. The earliest paths in the scientific research were focused on many crystalline materials, such as mica or feldspar. In the 50 s, the research was reoriented towards the elaboration materials. During the 60 s, the glass was selected by the international community as the confinement material of fission products solutions [2]. In order to dispose the high-level waste, many glassy matrices were selected: borosilicated, alumino-silicated, and alumino-borosilicated. They are a suitable solution, employed for a large spectrum of radionuclides [3].

The chemical composition of such glasses is a compromise between three goals, namely the chemical flexibility of the glass network, which will host more than 30 elements; the melting technological feasibility; and good waste package long-term behavior, which must ensure a safe confinement of radionuclides [2]. In order to minimize the number of waste packages, a glass with an adequate chemical composition, capable of sequestering high amounts of radionuclides per container, particularly lanthanides and actinides, is required. Such a glass should have both excellent chemical and self-irradiation durabilities.

Among the studied glasses, rare-earth element (REE)-rich glasses present such properties. However, from a technological point of view, their high synthesis temperatures ($T > 1450$°C) are a crippling criterion [3]. Adding to that, these glasses may induce undesired crystallizations during cooling, developing a concentration gradient between the amorphous and crystalline phases. Both the covalent and ionic interactions between ions in an oxides glass depend on the content of this last in REE elements. The alkali and alkaline-earth cations play several roles in the glass network, including hosting lanthanide ions in the vicinity of no-bridged oxygens (NBO), compensating the local excess of negative charges around Nd^{3+} bonds, etc. To achieve this, the bonds of REE elements in the glass network play a crucial role in glass dedicated to fission product (FP) immobilization, for the stability of a glass network under radioactive disintegrations. Water alteration of a glassy matrix is the main factor leading to radionuclide release in the environment. The second cause is the self-irradiation of the waste package [2].

To deal with this issue, many studies have focused on new chemical formulas of alumino-borosilicated glasses able to confine actinides, fission products, and Mo-reach wastes. In such glasses, the phase precipitations should be minimum. Thus, the glass network is thoroughly studied to elucidate the characteristics of both lanthanide and actinide bonds. This study deals with the synthesis and characterization of a Mo-reach alumino-borosilicated nuclear glass. This glass contains REE, simulating fission products, and variable Cs_2O contents. Cs is in its stable nonradioactive form. The glass is synthesized by a double melting at 1380°C. In

order to elucidate the glass microstructure, in particular Nd and Cs locations in the glass network, microstructural analyses such as X-ray diffraction (XRD) and both Raman and Fourier transform infrared (FTIR) spectroscopies are performed. The Nd valence is assessed by Raman spectroscopy.

Experimental. The chemicals employed in the synthesis are Al_2O_3 (Fluka), B_2O_3 (purity ≥ 99%), CaO (Merck, purity ≥ 97%), Fe_2O_3 (Merck, purity ≥ 99%), Li_2O (purity ≥ 99%), MoO_3 (Merck, purity ≥ 99.5%), Nd_2O_3 (Fluka, purity ≥ 99,9%), P_2O_5 (Merck, purity ≥ 98%), SiO_2 (Supelco Analytica), ZrO_2 (Aldrich, purity 99%), Na_2O (Merck, purity > 99%), ZnO (Labosi), Cs_2CO_3(Fluka), $Sr(NO_3)_2$ (BDH Chemicals, purity 99%), and Co_3CO_4 (Fluka, purity > 98%). The cobalt carbonate, Co_3CO_4, is calcined at 500°C in a BLF 1800 furnace during 5 h. The same furnace is used for the whole set of experiments.

The glass chemical composition is given in Table 1. All reagents are milled before weight. The glass synthesis is conducted according to the method of Vance et al. [4] method, with a batch of 60g glassy. The mixtures with different Cs_2O contents are homogenized during 5 h and then melted in Pt crucibles at 1380°C during 3 h, with a heating step of 6°C/min. The melts are poured in cylindrical molds, on graphite plates heated at 300°C, then annihilated at 600°C during 2 h. The glass cylinders are cut into slices in order to obtain slices of 3 to 4 mm in diameter. Some samples are milled in powders for analysis purposes.

TABLE 1. Chemical Composition (wt.%) of the Glass as a Function of the Cs_2O Content

Oxide	Glass1 [Cs_2O] = 0.3 wt.%	Glass 2 [Cs_2O] = 0.4, wt.%	Glass 3 [Cs_2O] = 0.6 wt.%
Na_2O	09.00	09.00	09.00
B_2O_3	13.00	13.00	13.00
Li_2O	03.00	03.00	03.00
Al_2O_3	07.00	07.00	07.00
MoO_3	10.00	10.00	10.00
P_2O_5	03.10	03.10	03.10
ZnO	05.00	05.00	05.00
ZrO_2	03.00	03.00	03.00
CaO	06.10	06.10	06.10
Cs_2O	0.30	0.40	0.60
SrO	00.70	00.70	00.70
Nd_2O_3	01.50	01.50	01.50
SiO_2	37.50	37.40	37.20
Fe_2O_3	00.60	00.60	00.60
Co_3CO_4	00.20	00.20	00.20
Total	100.00	100.00	100.00

The glass geometrical density is measured. Phase identification of the crystalline phases that may form in the glasses bulk is performed by XRD analysis with a monochromatic CuK_α Philips X'Pert Pro diffractometer, using Philips X'Pert Plus 2004 software. A nickel crystal was employed as an internal standard. The analysis parameters are: scanning rate 0.02°/s, counting time 1 s/step for 2θ varying from 10 to 100°, I = 40 mA, V = 45 kV, and λ = 1.5418 Å.

Phase identification is performed using X'Pert High Score software [5] and by comparison with the standard data of the Joint Committee for Powder Diffraction Standards (JCPDS).

The FTIR spectra are collected in the range 4000–1000 cm^{-1}, at room temperature, using a Nicolet 380 spectrometer. The analyses are performed on milled samples, mixed with KBr, and pelletized in the form of transparent films. The spectra are analyzed by OMNIC software.

Raman spectroscopy is performed using a LabRAM HR Evolution spectrometer provided with a blue laser (473 nm) as an excitation source, and a CCD detector. The Raman spectra are collected in the region 1500–100 cm^{-1}, with a spectral resolution of 0.3 cm^{-1}. Five accumulated scans are recorded for each spectrum, with an accumulation of 05 s. All experiments are performed at room temperature on glass slices of about 3–4 mm of thickness, with an ×100 μm confocal objective, at the laboratory of the research unit of materials sciences and applications of Constantine University 1.

Results and discussion. The synthesized glasses are blue, with a difference between the surface and the bulk, due to the hydration processes (Fig. 1). The glass density increases slightly with the Cs_2O content, between 1.96 and 2.75 (Table 2), and remains comparable with the value given in the literature (2.72) for an aluminosilicated glass obtained by a double melting at 1300°C [6].

Fig. 1. Morphological aspect of the synthesized glasses.

TABLE 2. Glass Densities as a Function of the Cs_2O Content

Cs_2O content, wt.%	0.3	0.4	0.6
Density, g/cm^3	1.96	1.42	2.75
REE and Morich glass [6]	2.72		

For the three Cs_2O contents, XRD diffractograms are gathered on Fig. 2. The glasses exhibit minor crystallizations phenomena. For 0.3 and 0.6 wt.% Cs_2O, a $CaMoO_4$ tetragonal powellite, of both 141/a space group and 88 number, associated to the JCPDS standard 01-085-0585 was identified. For the glass with 0.4 wt.% Cs_2O, traces of monoclinic SiO_2 crystalline phase were found, corresponding to the JCPDS standard 01-083-183, of Fe silicate $(Fe_3Al_2(SiO_4)_3$, corresponding to the JCPDS standard 01-085-2498, and of Sr-Nd-Fe oxide $SrNdFeO_4$, corresponding to the JCPDS 01-076-1876. Chouard et al. [7] have synthesized an alumino-borosilicate glass, containing 1.61 wt.% of Mo oxide and 3.59 wt.% of Nd-La oxide, at a 1300°C melting temperature. They found crystallization of $CaMO_4$ powellite in the glass bulk due to the weak solubility of Mo in the glass. This crystallization decreases by the addition of Nd_2O_3 and disappears for 8 wt.% content of Nd_2O_3. This proves the ability of Mo to induce crystallizations in Mo-rich alumino-borosilicate glasses.

The FTIR analysis gives the spectra shown in Fig. 3. The absorption band at 457.8 cm^{-1} is assigned to the vibration of Si-O-Si and O-Si-O in the glass. It is located at 464.2 cm^{-1} for the intermediate composition of 0.4 wt.% of Cs_2O [8]. The weak band at 680–690 cm^{-1} is assigned to BO_3 vibration. For borate glasses, it is located at 700 cm^{-1} [9]. Prasanta Kumar Ojhar reports the stretching vibration of B-O-B at 683 cm^{-1} [8]. Between 798 and 805 cm^{-1} the absorption band of Al-O-Al vibrations appears, attributed to the AlO_4 tetrahedral bond [10].

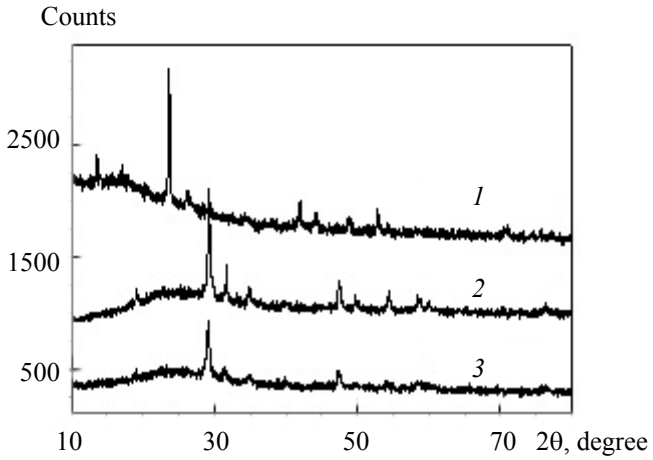

Fig. 2. Glasses diffractograms for different Cs_2O contents, [Cs_2O] = 0.6 (1), 0.4 (2), and 0.3 wt.% (3).

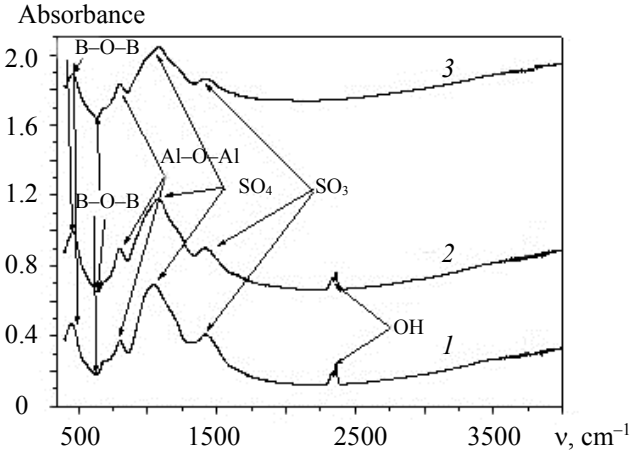

Fig. 3. Glass FTIR spectra as a function of the Cs_2O content, [Cs_2O] = 0.6 (1), 0.4 (2), and 0.3 wt.% (3).

For the glass containing 0.3 wt.% of Cs_2O, the vibration band at 1066 cm^{-1} can be attributed to the SiO_4 in a partially depolymerized network. This band is reported between 1030 and 1020 cm^{-1} [9]. This band shifts to 1099 and with a slight reversal to 1092 cm^{-1} with the Cs_2O content (0.4 and 0.6%, respectively), showing a certain network polymerization with increase in the Cs^+ content, and thus the decrease in NBO and the increase in BO (bridged oxygens). The band at 1422 cm^{-1} shifts to 1428 cm^{-1} when the Cs_2O content reaches 0.6 wt.%. This can be attributed to the asymmetrical stretching relaxation of the B-O bond in trigonal BO_3 units.

This band can appear in a large interval from 1200 to 1635 cm^{-1}, depending on the glass chemical composition [11]. The strong adjacent bands at 2350 and 2360 cm^{-1} show –OH bonds at the glass surface, proving the glass hydration ability at the surface, and thus their tendency to corrosion [10]. One can conclude that the addition of Cs_2O raises the polymerization degree of the glass network. Meanwhile, the network depolymerization affects the number of O-Si-O bonds. Raman spectroscopic analyses of the three glasses, in the spectral field between 300 and 1000 cm^{-1}, gave the spectra gathered in Fig. 4. The main identified vibrations bands are reported in Table 3.

The glasses Raman spectra for different Cs_2O contents show that the peaks recorded at 200 cm^{-1} present external vibration mode revealing crystallization into the glasses. The band located at 700 cm^{-1} belongs to both the SiO_4 and AlO_4 stretch massif. It is strong for 0.3 wt.% Cs_2O, and attenuated for 0.4 and 0.6 wt.% of Cs_2O [12]. Moreover, it shifts from the region of 850–1300 to 680–900 cm^{-1} for large Mo glass contents, thus disturbing the rearrangement of Ca and Na. This does not affect the Cs_2O solubility in the glass. For steric reasons, Cs is larger than the other alkali/alkaline-earth elements. It can affect the cation distribution around SiO_4.

TABLE 3. The Main Raman Vibrations Bands (cm^{-1}) Identified in the Studied Glasses

Vibration mode	Raman band	Vibration band [6]
$CaMoO_4$		
ν_1 ($2A_1$)	877	879, 892
ν_3 ($2F_2$)	844, 792	848, 795
ν_4 ($2F_2$)	387	407, 393
ν_2 ($2E$)		
$\nu_{f.r}$ ($2F_1$) free rotation	319	324
ν_{ext} external modes MoO_2^{-4} and Ca^{2+}	200	208
SiO_4 vibrations		
SiO_4	844	800–840
Q1	1050–1070	900–1100
Q2	900	950, 1150–1250
Q3	1000	1070
Q4	1070	1130

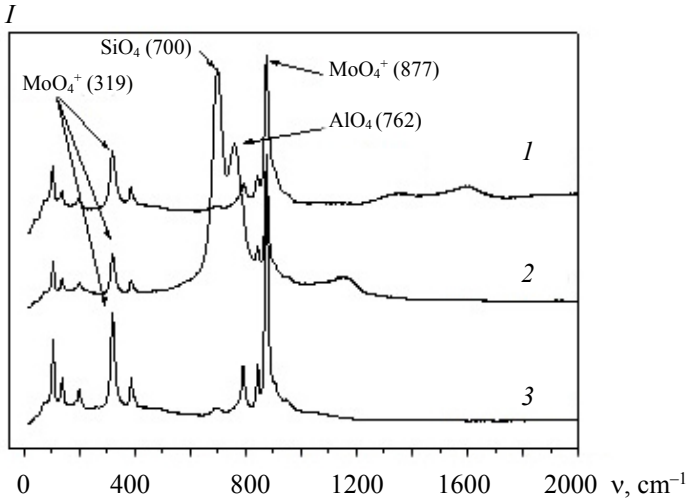

Fig. 4. Glass Raman spectra as a function of the Cs_2O content, [Cs_2O] = 0.6 (1), 0.4 (2), and 0.3 wt.% (3).

The distribution of nanometric tetrahedral SiO_4 of the silicate network embedding K, Na, and Ca is observed between 700 and 1300 cm^{-1} (stretching modes of Si-O bonds in SiO_4 tetrahedra) [13]. The different types of SiO_4 are different in their connection modes: Q_0 is a single tetrahedron, Q_1, is a tetrahedron bonded to a neighbor by a Si-O-Si bridge, Q_2 is a tetrahedron linked to two neighbors by two Si-O-Si bridges, etc. The band around 1050–1070 cm^{-1} is assigned to symmetrical stretching vibrations of the glass SiO_4 (units Q_n) tetrahedra. For a given M_2O alkali oxide, the distribution of Q_n unit scan varies with the alkali nature in the glass. This effect can be explained in terms of the equilibrium displacement in the melt ($2Q_n \leftrightarrow Q_{n-1}+Q_{n+1}$, n = 3, 2, 1), which depends on the strength field of the alkali ion.

This is considerable for lithium element, which is able to induce phase separations [14]. The weak band at 1000 cm^{-1} is assigned to Q_3 units that host Nd^{3+} ions in their vicinity [16]. Moreover, a Raman spectroscopic study of the evolution of Q_n unit concentrations as a function of temperature reveals that the balance is moved towards the right with rise in temperature for contents deviating from the separation field [15].

In the region from 1300 to 1500 cm^{-1} the stretching vibrations of BO_3 units appear. The bands located at 319, 792, and 844 cm^{-1} attributed to symmetrical stretching vibrations of the glass MoO_4^{2-} tetrahedral entities. The band located at 792 cm^{-1} is strong for 0.3 wt.% Cs_2O content, compared to 0.4 and 0.6 wt.% Cs_2O content, proving that a weak rise in the Cs_2O content disturbs the glass network. The band located at 844 cm^{-1} is displaced. It is reported at 838 cm^{-1} in [17]. In general, the three peak shifts are due to the increase in the glass Cs_2O content, Cs_2O being less soluble in the glass. The band at 877 cm^{-1}, very strong whatever the Cs_2O content, is assigned to the contribution of the asymmetric stretching bands of the $[MoO_4]^{2-}$ tetrahedra in the glass structure.

These Raman bands are associated with the MoO_4^{2-} vibrations in $CaMoO_4$ powellite crystals identified in XRD analysis. The field of occurrence of molybdates and thus powellite is between 319 and 900 cm^{-1} with a maximum of crystallization located around 838 cm^{-1}. It agrees with the results reported in the literature for both HTC and R7T7 glasses [18]. These results demonstrate the Mo incorporation in the glass network during the glass fabrication process.

In order to elucidate the Nd and other REE environment in the glass bulk, it is important to determine the nature of oxygen atoms in the Nd^{3+} first coordination sphere (bridging oxygen (BO) or NBO) [6]. When BO atoms are present in the first coordination layer of Nd, it has been demonstrated by EXAFS analysis that the Nd-O bond length varies (2.42–2.47 Å); and the Nd-O bond valence varies between 0.44 and 0.39. This proves that the BO oxygen is a linked one, its valence being between 2.46 and 2.41 (which is higher than 2). Thus, Nd should be linked to seven to eight NBO oxygens. The resulting excess of negative charge will be compensated by modifying ions (Na^+ and/or Ca^{2+}). The number of Ca^{2+} in the Nd environment increases with the glass Ca content. Corradi et al. [19] have performed a molecular dynamic modeling study of the SiO_2-Na_2O-Nd_2O_3 system. They found that the REE elements near the environment are mainly constituted by NBO oxygens, which is in accordance with the EXAFS results. These authors found a relatively short Nb-O bond length (2.32 Å).

Conclusions. This study deals with the structural changes in Mo-rich alumino-borosilicate glass, dedicated to both Cs_2O and Mo containing radioactive waste. The synthesis is conducted by a double melting at 1380°C followed by an annealing at 600°C. Neodymium is an actinide surrogate. The glasses geometrical density increases with the Cs_2O content from 1.96 to 2.75 g/cm^3. XRD analysis shows the amorphous feature of the glasses, with traces of $CaMoO_4$ powellite, formed during cooling. FTIR analysis shows similar glass compositions. The main identified chemical bonds are Si-O-Si and O-Si-O of SiO_4, B-O-B of BO_3, and Al-O-Al of AlO_4. The addition of Cs_2O raises the polymerization rate in the glass network and thus decreases the number of NBO oxygens to the detriment of BO oxygens. Raman spectroscopic analysis shows that the Mo environment is less affected by the Cs_2O addition. It reveals the bands ascribed to MoO_4^{2-} in $CaMoO_4$ powellite. This demonstrates the addition of Mo to the crystalline phase during the synthesis process.

The stretching massive of SiO_4 and AlO_4 tetrahedra is influenced by the Mo great content. It is attenuated when the Cs_2O content reaches 0.4 wt.%, disturbing the Ca and Na distribution; Cs atoms remain soluble in the glass network. This proves that a slight increase in the Cs_2O content inhibits the crystallization of molybdate phases (Na_2MoO_4 and $CaMoO_4$). These results highlight the fact that the glass structure and the phase separation ability of molybdates phases depend on the REE oxide concentration and on the nature of alkali/alkaline-earth elements in the glass composition. There is no evident change in the lanthanide valence, which are probably in a $^{+}$III oxidation state. The cohesion of the glass network is still an issue when adding Cs_2O to its chemical composition. However, 6 wt.% of Cs_2O was added in the present studied glass without compromising the glass structure.

REFERENCES

1. O. Méplan, A. Nuttin. *La Gestion des Déchets Nucléaires. Images de la Physique*, Ed. Orsay, France, 9–17 (2006).
2. *Le Conditionnement des Déchets Nucléaires*, Rapport CEA, CEA, France, 27–70 (2016).
3. D. Caurant, I. Bardez, P. Loiseau, *J. Mater. Sci.*, **42**, 10203–10218 (2007).
4. E. R. Vance, J. Davis, K. Olufson, D. J. Gregg, M. G. Blackford, G. R. Griffiths, I. Farnan, J. Sullivan, D. Sprouster, C. Campbell, J. Hughes, *J. Nucl. Mater*., **448**, 325–329 (2014).
5. Philips X'pert High Score Package, diffraction Data CD-ROM, International center for diffraction Data, Newtown Square, PA (2004).
6. A. Quintas, *Etude de la structure et du comportement en cristallisation d'un verre nucléaire d'aluminoborosilacate de terre rare*, PhD Thesis, Pierre and Marie Curie University, Paris VI, France (2007).
7. N. Chouard, D. Caurant, O. Majerus, J. L. Dussossoy, S. Klimin, D. Pytalev, R. Baddour-Hadjean, J. P. Pereira-Ramos, *J. Mater. Sci*., **50**, 219–241 (2015).
8. P. K. Ojha, S. K. Rath, T. K. Chongdar, N. M. Gokhale, A. R. Kulkarni, *New J. Glass Ceram.*, **1**, 21–27 (2011).
9. E. Kashchieva, I. Petrov, L. Aleksandrov, R. Iordanova, Y. Dimitriev, *Phys. Chem. Glasses-B*, **53**, 264–270 (2012).
10. C. R. Gautam, A. Kumar Yadav, *OPJ*, **3**, 1–7 (2013).
11. C. Gautam, A. K. Yadav, A. K. Singh, *ISRN Ceram.*, **2012**, 17 (2012).
12. D. R. Neuville, L. Cormier, B. Boizot, A.-M. Flank, *J. Non-Cryst. Solids*, **323**, 207–213 (2003).
13. Ph. Colomban, J. Corset, *J. Raman Spectrosc.*, **30**, 863–866 (1999).
14. F. Angeli, J. M. Delaye, T. Charpentier, J. C. Petit, D. Ghaleb, P. Faucon, *J. Non-Cryst. Solids*, **276**, 132–134 (2000).
15. N. Ollier, T. Charpentier, B. Boizot, G. Wallez, D. Ghaleb, *J. Non-Cryst. Solids*, **341**, 26–34 (2004).
16. T. Schaller, J. F. Stebbins, M. C. Wilding, *J. Non-Cryst. Solids*, **243**, 146–157 (1999).
17. K. Brinkman, K. Fox, J. Marra, J. Reppert, J.Crum, M. Tang, *J. Alloys Compd*., **551**, 136–142 (2013).
18. N. Chouard, *Structure, stabilité thermique et résistance sous irradiation externe de verres aluminoborosilacates riches en terres rares et en molybdène*, PhD Thesis, Pierre and Marie Curie University-Paris VI, France (2011).
19. A. B. Corradi, V. Cannillo, M. Montorsi, C. Siligardi, A. N. Cormack, *J. Non-Cryst. Solids*, **351**, 1185–1191 (2005).